Probing Higher Orbital Angular Momentum of Laguerre-Gaussian Beams via Diffraction through a Translated Single Slit

Jadze Princeton C. Narag* and Nathaniel Hermosa
National Institute of Physics, University of the Philippines, Diliman, Quezon City 1101, Philippines

(Received 27 November 2018; revised manuscript received 28 February 2019; published 9 May 2019)

Laguerre-Gaussian (LG) beams and their orbital angular momentum (OAM) have found a plethora of applications—from quantum information to gravitational-wave detection. In this work, we probe the OAM of LG beams by using a digital micromirror device programmed as a single slit. We observe the diffraction patterns of the beams through the slit and we show that we can determine the OAM of the incoming beams from the changes in the diffraction pattern as the slit is moved transversely. Moreover, we demonstrate that we can access higher OAM modes compared to previous works involving slit diffraction. Our results are valuable in the study of OAM especially for beams where the current technology for detection is not yet mature, for example, beams whose wavelengths are in the terahertz regime or beams of higher energy such as, electron vortex beams.

DOI: 10.1103/PhysRevApplied.11.054025

I. LG BEAMS AND THE ORBITAL ANGULAR MOMENTUM OF LIGHT

Light has been shown by Woerdman *et al.* [1] to carry orbital angular momentum (OAM) as a consequence of its spatial structure. In particular, light beams possessing an azimuthal phase dependence of $\exp(i\ell\phi)$ where ℓ is an integer, carry OAM of $\ell\hbar$ per photon [2,3]. The canonical example of an OAM-carrying beam is the Laguerre-Gauss (LG) beam with an electric field given by [4]

$$u_\ell^p(\rho,\phi,z) \approx \left(\frac{\rho}{\omega}\right)^{|\ell|} L_p^{|\ell|}\left(\frac{2\rho^2}{\omega^2}\right) \exp\left(\frac{-\rho^2}{\omega^2}\right) \exp\left(i\ell\phi\right), \tag{1}$$

where ω is the beam waist, $L_p^\ell(2\rho^2/\omega^2)$ is the associated Laguerre polynomial, ℓ is the azimuthal mode, and p is the radial mode. The discontinuity of the azimuthal phase leads to a singularity or vortex at the center of the beam. The azimuthal mode ℓ, also called the topological charge, defines size of the vortex while p defines the number of radial nodes. The OAM of the LG beam has led to its applications in quantum information [5–11], micromachining [12,13], optical communication [14–17], optical tweezing [18–20], and in astronomy and gravitational-wave detection [21,22].

Common methods to measure OAM include interferometry [23–27] of the OAM beams with other structured beams and holography coupled with mode detectors and optical fibers. Moreover, the diffraction of the beam through different apertures has been shown to also be a practicable method of probing the OAM. For example, the diffraction of the LG beam through polygonal apertures [28–32] and multipinhole setups [33,34] are shown to be effective in probing their OAM. The classical single-slit [35,36] and double-slit [37,38] diffraction also have been re-examined using LG beams instead of the ordinary Gaussian beam. However, in these works the authors used stationary slits and were only able to probe the low-ordered modes. In this paper, we study the diffraction of the LG beam through a dynamic single slit using a digital micromirror device. We look at the fringe patterns formed and show that these are related to the topological charge of the LG beam. We explain the resulting structure of the diffraction by the method established in Ref. [39], of looking at the phase difference between the boundary of the slit. Our results are valuable in the study of OAM especially for beams where the current technology for detection is not yet mature, for example, beams whose wavelengths are in the terahertz regime or beams of higher energy, such as electron vortex beams [40,41]. In these, regimes, sophisticated devices, such as optical fibers, photonic crystals, spatial light modulators and CCD cameras, that can be used to detect OAM, are still rare. But we can certainly use slits and observe diffraction effects for all wavelength and energy ranges to probe the OAM and other properties of a beam.

II. LG BEAM DIFFRACTION THROUGH A MOVABLE SLIT

The main assumption of the classical single-slit experiment is that a plane wave impinges on the slit. That is, at the plane of the slit the waves are in phase. The resulting

*jadzenarag@gmail.com

diffraction pattern can be derived by imagining secondary sources along the slit. The phase difference between these wavelets are caused by their path difference to the observation point. Mathematically, the field is given by the Huygens diffraction integral,

$$u = \iint_S \frac{ik}{r} e^{ikr} dS, \tag{2}$$

where r is the distance from the source point to the observation point, k is the wavevector, and the integral is over the entire surface S containing the source points. Applying the conditions for the Fraunhofer approximations and taking the intensity gives [42]

$$I \propto \text{sinc}^2(\beta), \tag{3}$$

where $\beta = kt\sin\theta/2$, t being the thickness of the slit, and θ the angle from the center of the slit to the observation point. The sinc function means that there are alternating bright and dark fringes perpendicular to the slit.

If instead we use a higher-order LG beam rather than a Gaussian beam, there is an additional phase difference due to the azimuthal phase dependence of the LG beam and the waves are no longer in phase in the plane of the slit. This additional phase difference can be incorporated inside the exponential in Eq. (2). However, evaluating the integral can be a bit involved so instead we use the technique established in Ref. [39]. In that paper, where diffraction of a Gaussian beam through slits shaped as polygons were describe using caustics and catastrophe optics, we argued that we can consider only the vertices of the polygonally shaped slits because at these exceptional points the integral in Eq. (2) is discontinuous and there in an incomplete cancellation of phase [39,43]. For a vertical single slit, the concept of a vertex is ill defined but it does have exceptional points at the top and at the bottom end of the slit and we can consider the phase difference between these points to predict the diffraction pattern.

In the case of LG beams, the phase on the top and bottom edge of the slit differs depending on the OAM and on the position x of the slit with respect to the center of the beam. A simple calculation shows that the phase difference $\Delta\phi$ between the top and bottom edge of the slit is given by

$$\Delta\phi = 2\ell \cos^{-1}\left(\frac{x}{\sqrt{x^2+L^2}}\right), \tag{4}$$

where ℓ is the topological charge of the beam, x is the displacement of the slit, and $2L$ is the length of the slit. The definition of these variables are illustrated in Fig. 2. There is destructive interference and constructive interference when the phase difference is an odd and even multiple of π, respectively—and this depends on both the position of the slit and the OAM of the beam. For a stationary slit

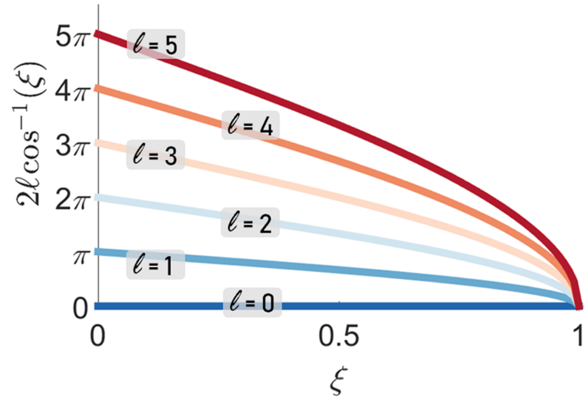

FIG. 1. $2\ell\cos^{-1}$ vs ξ. Here ξ is a normalized distance, $\xi = x/\sqrt{x^2+L^2}$. The phase difference transitions from an odd to even (or even to odd) multiples of π as the slit position x becomes very large or as ξ approaches 1. The number of transitions, from odd to even or even to odd multiples of π depends on the OAM of the beam.

at $x = 0$, the phase difference $\Delta\phi = \ell\pi$ and this configuration can distinguish between odd and even ℓ values. The central fringe is bright when ℓ is odd and it is dark when ℓ is even. We can further probe the magnitude of the OAM by moving the slit transversely. Figure 1 shows the trend of the phase difference as the slit is moved away from the center.

As the slit is moved to the center, the phase difference decreases and transitions from an odd to even multiple of π when the OAM is odd, and from odd to even multiple of π when the OAM is even. Consequently, the intensity of the fringe transitions from dark to bright or dark to bright depending on whether ℓ is odd or even. We can therefore probe the OAM by observing the variation in the intensity

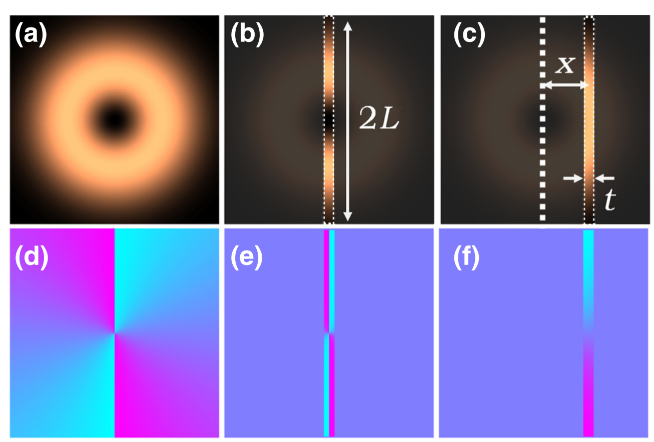

FIG. 2. Slit modulation. The intensity of the LG_2 beam before the slit (a), immediately after the slit (b), and when the slit is translated by a distance x (c). (d)–(f) The corresponding phase distribution.

as the slit is moved. Furthermore, the number of transitions and rate of these transitions differ for various ℓ's. In general, the central fringe starts as a dark band for odd ℓ and a bright band for even ℓ and the evolution is faster for larger ℓ.

III. METHODOLOGY

We simulate the generation of LG_ℓ^0 beams by approximating the beams using Eq. (1). The beams are then modulated in amplitude by a slit of thickness = 54 μm. This is done by multiplying the beam matrix element wise with the amplitude mask of the slit. The intensity of $|LG|^2$ beam (a) before the slit, (b) after the slit, and (c) after the slit has been moved laterally are shown in Figs. 2(a)–2(c), respectively. The corresponding phases are shown in Figs. 2(d)–2(f).

The field right after the slit is then Fourier transformed to simulate the effect of the slit being placed in the back focal plane of a lens and being imaged in the front focal plane.

The experiment is realized using the setup in Fig. 3. A 632.8-nm HeNe laser is collimated by lenses L1 and L2. The beam is then converted into LG beams of various topological charges by uploading their corresponding phase profiles into the spatial light modulator. A digital micromirror device (DMD) is then used as a dynamic slit. The DMD is composed of an array of 608 by 608 mirrors of dimension 10.8 μm and is controllable through a computer. The slit is moved from -1 mm (left) to 1 mm (right) of the beam center. The slit thickness is 54 μm. Finally, the diffraction is focused using lens L3 with focal length 25 cm and is captured using a CCD camera in the back focal plane of L3. The aperture after the spatial light modulation (SLM) is used only to block the higher-order modes. This aperture does not contribute any significant diffraction effects since it is a relatively large aperture (2 cm diameter).

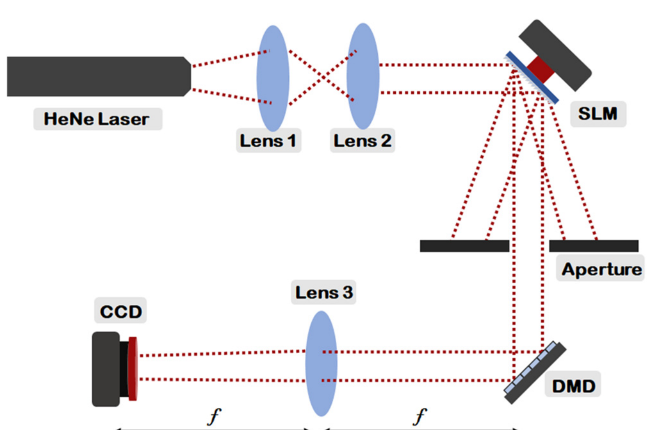

FIG. 3. Experimental setup. The LG beams are produced by uploading their phase in the SLM. We are able to vary the position of the single slit by using a DMD as a dynamic slit. The diffraction is imaged in the far field using a CCD camera.

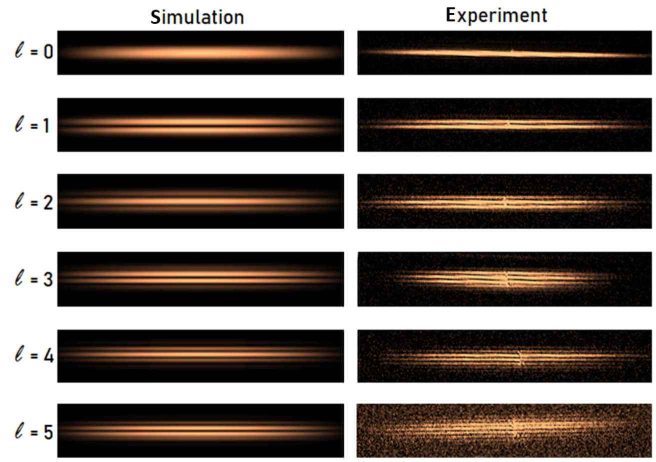

FIG. 4. Diffraction through a single slit of LG_0^ℓ. For odd ℓ there is a central horizontal dark band while for even ℓ the central horizontal band is bright.

The diffraction patterns when $x = 0$ in Fig. 4 show an obvious difference between the LG beams with odd and even ℓ. There is a horizontal dark line that cuts through the center of diffraction pattern for odd ℓ while for even ℓ the central horizontal band is bright. The number of fringes is also proportional to ℓ. In particular, the number of fringes is $\ell + 1$, the same as the result in Ref. [44]. For higher ℓ's, however, it becomes more difficult to resolve the fringes. Also, the diffraction pattern becomes darker overall for larger ℓ's since the vortex is also larger. That is why in the experimental result for $\ell = 5$ in Fig. 4, we increase the camera sensitivity to be able to capture the diffraction pattern and the images are noiser with more grains.

As the slit is moved, we graphed the intensity of the central horizontal fringe in Fig. 5. The central intensity when $x = 0$ for LG beams with odd (even) ℓ's start at a minima (maxima). When the slit is moved, the central horizontal band changes from an intensity maxima (minima) to a minima (maxima) for even (odd) ℓ. This is explained by the variation of $\Delta\phi$ with respect to the slit position in Eq. (4). The graph of Eq. (4) shows that for odd ℓ, the phase difference starts as an odd multiple of π and alternately becomes an even then odd multiple of π as the slit displacement becomes very large. For even ℓ, the phase difference also alternates between odd and even multiples of π but it starts, at $x = 0$, as an even multiple. This means that the number of intensity changes, from maxima to minima (or minima to maxima), and how fast these changes occur, as a function of slit position, are dependent of ℓ. For example, for $\ell = 1$, the phase difference changes from an odd to an even multiple of π only once. Thus the central intensity only goes once from a dark to a bright fringe. The rates are also faster for larger ℓ. We see in Fig. 4 that for

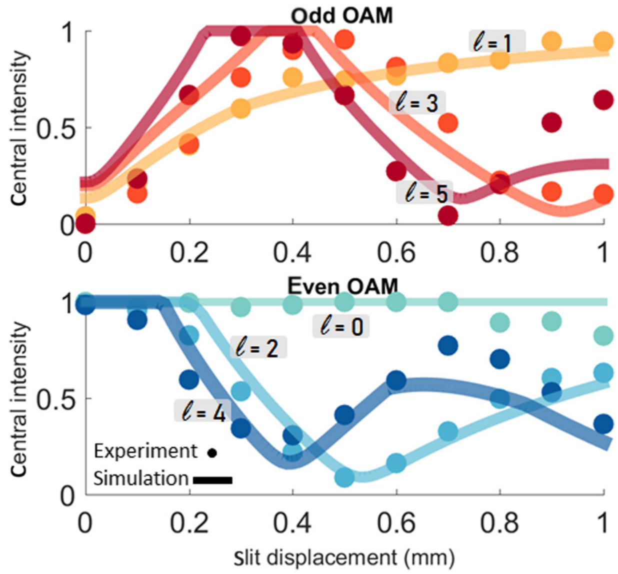

FIG. 5. Central intensity vs slit position x. The central intensity for odd (even) ℓ's start from a minima (maxima) and then changes to a maxima (minima) as the slit is moved from the center. Larger ℓ's evolve faster than smaller ℓ's.

odd ℓ the central intensities are minima when $x = 0$, but as we displace the slit the graph for $\ell = 5$ evolves faster than that of $l = 3$ and that $\ell = 3$ is faster than that of $\ell = 1$. The analogous behavior is observed for even ℓ's: $\ell = 4$ evolves faster than $\ell = 2$, which evolves faster than $\ell = 0$.

IV. RESULTS AND DISCUSSIONS

The diffraction of LG beams through single slits to probe their OAM have been examined before. In Ref. [36], the single-slit diffraction of OAM beams is analyzed by taking the phase difference between the edge of the short axis of the slit. That is, the slit has some finite thickness. The analysis in Ref. [36] essentially treats the single slit as a double slit. The result is that the fringes are not straight but are bent. In fact, the same technique is used in Ref. [38] and in Ref. [37] for double slits and found the same bending of the fringes. Here, bending is not noticable since we used a very thin slit. For a very thin and long slit, the effect that there is a central minima and maxima for odd and even ℓ is more evident than the bending of the fringes. In another paper, Ferreira *et al.* [35] analyzed the diffraction of the LG beam through a single slit in terms of the phase difference between the end of the long axis of the slit. They explained the resulting pattern by approximating the LG beam by two separate Gaussian beams. In these previous works, the OAM of LG beams were determined by simply looking at the diffraction patterns through stationary slits and counting the number of fringes in the pattern as in Fig. 4. However, it becomes harder and harder to resolve the fringes just by looking at the diffraction pattern. Our method of using a dynamic slit and observing the changes in the diffraction allows easier probing of higher OAM values—it is easier to determine the OAM from Fig. 5 than from Fig. 4. We quantify the contrast of the fringes using the visibility $v = I_{\max} - I_{\min}/I_{\max} + I_{\min}$. The visibilities of the fringes of the diffraction patterns are [0.6431, 0.6039, 0.5255, 0.4745, 0.4314, 0.4078] for $\ell = 0$ to 5, respectively; while the visibilities of the transitions in our results in Fig. 5 are [0.3215, 0.9259, 0.8387, 1, 0.8157, 1] for $\ell = 0$ to 5. The visibility of the fringes reduces greatly for higher OAM values since the central dark spot of the beams increases as ℓ and the images becomes darker—while the visibility for our method remains high even for $l = 5$. It must be noted, however, that the visibility for $l = 0$ for our method is low since this is a flat graph and the intensity does not change as position.

In our setup, the DMD can also be replaced with the slit placed in the motor that translates the slit, which may provide a better resolution in position. Using a DMD, however, has several advantages: we can easily change the position on demand; the dimensions of the slit can also be programmed to the desired width and length; and that there is no misalignment that may be due to mechanical movement such as wobbling inherent to mechanical translation and of hysteresis. In Ref. [44], the slit is translated along the optical axis to investigate the effect of the quadratic radial variation of phase in LG beams. A limitation common to all techniques using a single slit is that it cannot distinguish between the handedness of the OAM. It can only determine the absolute value of the OAM but not whether it is positive or negative.

V. CONCLUSION

We demonstrate that the OAM of an LG beam can be determined by looking at its diffraction through a single slit. We derive the difference between the endpoints of the slit and we show that for odd ℓ there is a central minima and for an even ℓ there is a central maxima. Furthermore, we also investigate the evolution of this phase difference as the slit is moved transversely. We used a digital micromirror device as a dynamic slit whose position can be controlled through a computer. We show that although OAM of the slit can be determined using stationary slits, with a dynamic slit we can access higher OAM values by looking at how the central horizontal fringes evolve as we change the slit position. We find that the evolution from intensity minima to maxima or maxima to minima is faster for larger ℓ.

ACKNOWLEDGMENTS

The authors acknowledge the Office of the Chancellor of the University of the Philippines Diliman through the Office of the Vice Chancellor for Research and Development Outright Research Grant for funding support. N.H.

is a recipient of the Balik PhD Program of the Office of the Vice President for Academic Affairs of the University of the Philippines. J.N. is a Science Research Specialist of the PCIEERD Project No. 04002 under the Department of Science and Technology of the Republic of the Philippines.

[1] L. Allen, M. W. Beijersbergen, R. J. C. Spreeuw, and J. P. Woerdman, Orbital angular momentum of light and the transformation of Laguerre-Gaussian laser modes, Phys. Rev. A **45**, 8185 (1992).

[2] Halina Rubinsztein-Dunlop *et al.*, Roadmap on structured light, J. Opt. **19**, 013001 (2016).

[3] Miles J. Padgett, Orbital angular momentum 25 years on, Opt. Express **25**, 11265 (2017).

[4] Bahaa E. A. Saleh and Malvin Carl Teich, *Fundamentals of Photonics* (John Wiley & Sons, Amsterdam, Netherlands, 2019).

[5] Alicia Sit, Robert Fickler, Fatimah Alsaiari, Frédéric Bouchard, Hugo Larocque, Patrick Gregg, Lu Yan, Robert W. Boyd, Siddharth Ramachandran, and Ebrahim Karimi, Quantum cryptography with structured photons through a vortex fiber, Opt. Lett. **43**, 4108 (2018).

[6] Robert Fickler, Radek Lapkiewicz, Marcus Huber, Martin P. J. Lavery, Miles J. Padgett, and Anton Zeilinger, Interface between path and orbital angular momentum entanglement for high-dimensional photonic quantum information, Nat. Commun. **5**, 4502 (2014).

[7] Mohammad Mirhosseini, Omar S. Magaña-Loaiza, Malcolm N. O'Sullivan, Brandon Rodenburg, Mehul Malik, Martin P. J. Lavery, Miles J. Padgett, Daniel J. Gauthier, and Robert W. Boyd, High-dimensional quantum cryptography with twisted light, New J. Phys. **17**, 033033 (2015).

[8] Manuel Erhard, Robert Fickler, Mario Krenn, and Anton Zeilinger, Twisted photons: New quantum perspectives in high dimensions, Light: Sci. Appl. **7**, 17146 (2018).

[9] Gabriel Molina-Terriza, Juan P. Torres, and Lluis Torner, Management of the Angular Momentum of Light: Preparation of Photons in Multidimensional Vector States of Angular Momentum, Phys. Rev. Lett. **88**, 013601 (2001).

[10] Juan P. Torres, Yana Deyanova, Lluis Torner, and Gabriel Molina-Terriza, Preparation of engineered two-photon entangled states for multidimensional quantum information, Phys. Rev. A **67**, 052313 (2003).

[11] Stanislav Straupe and Sergei Kulik, Quantum optics: The quest for higher dimensionality, Nat. Photonics **4**, 585 (2010).

[12] Gianluca Ruffato, Michele Massari, Marta Carli, and Filippo Romanato, Spiral phase plates with radial discontinuities for the generation of multiring orbital angular momentum beams: Fabrication, characterization, and application, Opt. Eng. **54**, 111307 (2015).

[13] Kosta Ladavac and David G. Grier, Microoptomechanical pumps assembled and driven by holographic optical vortex arrays, Opt. Express **12**, 1144 (2004).

[14] Nenad Bozinovic, Yang Yue, Yongxiong Ren, Moshe Tur, Poul Kristensen, Hao Huang, Alan E. Willner, and Siddharth Ramachandran, Terabit-scale orbital angular momentum mode division multiplexing in fibers, Science **340**, 1545 (2013).

[15] Graham Gibson, Johannes Courtial, Miles J. Padgett, Mikhail Vasnetsov, Valeriy Pas'ko, Stephen M. Barnett, and Sonja Franke-Arnold, Free-space information transfer using light beams carrying orbital angular momentum, Opt. Express **12**, 5448 (2004).

[16] Jian Wang, Jeng-Yuan Yang, Irfan M. Fazal, Nisar Ahmed, Yan Yan, Hao Huang, Yongxiong Ren, Yang Yue, Samuel Dolinar, Moshe Tur, and Alan Willner, Terabit free-space data transmission employing orbital angular momentum multiplexing, Nat. Photonics **6**, 488 (2012).

[17] A. E. Willner, H. Huang, Y. Yan, Y. Ren, N. Ahmed, G. Xie, C. Bao, L. Li, Y. Cao, Z. Zhao, J. Wang, M. P. J. Lavery, M. Tur, S. Ramachandran, A. F. Molisch, N. Ashrafi, and S. Ashrafi, Optical communications using orbital angular momentum beams, Adv. Opt. Photonics **7**, 66 (2015).

[18] Grover A. Swartzlander, Erin L. Ford, Rukiah S. Abdul-Malik, Laird M. Close, Mary Anne Peters, David M. Palacios, and Daniel W. Wilson, Astronomical demonstration of an optical vortex coronagraph, Opt. Express **16**, 10200 (2008).

[19] David G. Grier, A revolution in optical manipulation, Nature **424**, 810 (2003).

[20] H. He, M. E. J. Friese, N. R. Heckenberg, and H. Rubinsztein-Dunlop, Direct Observation of Transfer of Angular Momentum to Absorptive Particles from a Laser Beam with a Phase Singularity, Phys. Rev. Lett. **75**, 826 (1995).

[21] Gregory Foo, David M. Palacios, and Grover A. Swartzlander, Optical vortex coronagraph, Opt. Lett. **30**, 3308 (2005).

[22] Massimo Granata, Christelle Buy, Robert Ward, and Matteo Barsuglia, Higher-order Laguerre-Gaussmode generation and interferometry for gravitational wave detectors, Phys. Rev. Lett. **105**, 231102 (2010).

[23] M. S. Soskin, V. N. Gorshkov, M. V. Vasnetsov, J. T. Malos, and N. R. Heckenberg, Topological charge and angular momentum of light beams carrying optical vortices, Phys. Rev. A **56**, 4064 (1997).

[24] I. V. Basistiy, V. Yu. Bazhenov, M. S. Soskin, and M. Vu. Vasnetsov, Optics of light beams with screw dislocations, Opt. Commun. **103**, 422 (1993).

[25] I. V. Basistiy, M. S. Soskin, and M. V. Vasnetsov, Optical wavefront dislocations and their properties, Opt. Commun. **119**, 604 (1995).

[26] M. Harris, C. A. Hill, P. R. Tapster, and J. M. Vaughan, Laser modes with helical wave fronts, Phys. Rev. A **49**, 3119 (1994).

[27] M. Padgett, J. Arlt, N. Simpson, and L. Allen, An experiment to observe the intensity and phase structure of Laguerre–Gaussian laser modes, Am. J. Phys. **64**, 77 (1996).

[28] Juarez G. Silva, Alcenísio J. Jesus-Silva, Máarcio A. R. C. Alencar, Jandir M. Hickmann, and Eduardo J. S. Fonseca, Unveiling square and triangular optical lattices: A comparative study, Opt. Lett. **39**, 949 (2014).

[29] Anindya Ambuj, R. Vyas, and Surendra Singh, Diffraction of orbital angular momentum carrying optical beams by a circular aperture, Opt. Lett. **39**, 5475 (2014).

[30] J. M. Hickmann, E. J. S. Fonseca, W. C. Soares, and S. Chávez-Cerda, Unveiling a Truncated Optical Lattice Associated with a Triangular Aperture using Light's Orbital Angular Momentum, Phys. Rev. Lett. **105**, 053904 (2010).

[31] A. Mourka, J. Baumgartl, C. Shanor, K. Dholakia, and E. M. Wright, Visualization of the birth of an optical vortex using diffraction from a triangular aperture, Opt. Express **19**, 5760 (2011).

[32] Luś E. E. de Araujo, and Matthew E. Anderson, Measuring vortex charge with a triangular aperture, Opt. Lett. **36**, 787 (2011).

[33] Lei Shi, Linghao Tian, and Xianfeng Chen, Characterizing topological charge of optical vortex using non-uniformly distributed multi-pinhole plate, Chin. Opt. Lett. **10**, 120501 (2012).

[34] Gregorius C. G. Berkhout, and Marco W. Beijersbergen, Method for Probing the Orbital Angular Momentum of Optical Vortices in Electromagnetic Waves from Astronomical Objects, Phys. Rev. Lett. **101**, 100801 (2008).

[35] Queila S. Ferreira, Alcenísio J. Jesus-Silva, Eduardo J. S. Fonseca, and Jandir M. Hickmann, Fraunhofer diffraction of light with orbital angular momentum by a slit, Opt. Lett. **36**, 3106 (2011).

[36] Devinder Pal Ghai, P. Senthilkumaran, and R. S. Sirohi, Single-slit diffraction of an optical beam with phase singularity, Opt. Lasers Eng. **47**, 123 (2009).

[37] Olivier Emile and Janine Emile, Young's double-slit interference pattern from a twisted beam, Appl. Phys. B **117**, 487 (2014).

[38] H. I. Sztul and R. R. Alfano, Double-slit interference with Laguerre-Gaussian beams, Opt. Lett. **31**, 999 (2006).

[39] J. Narag and N. Hermosa, Diffraction of polygonal slits using catastrophe optics, J. Appl. Phys. **124**, 034902 (2018).

[40] Masaya Uchida and Akira Tonomura, Generation of electron beams carrying orbital angular momentum, Nature **464**, 737 (2010).

[41] Johan Verbeeck, He Tian, and Peter Schattschneider, Production and application of electron vortex beams, Nature **467**, 301 (2010).

[42] Max Born and Emil Wolf, *Principles of Optics: Electromagnetic Theory of Propagation, Interference and Diffraction of Light* (Elsevier, Hobokon, New Jersey, 2013).

[43] Riccardo Borghi, Catastrophe optics of sharp-edge diffraction, Opt. Lett. **41**, 3114 (2016).

[44] Anindya Ambuj, Hsiao-Harng Shiau, Mike Lucini, Reeta Vyas, and Surendra Singh, in *Frontiers in Optics 2011/Laser Science XXVII* (Optical Society of America, 2011), p. LThC3.